Journal of Colloid and Interface Science **243,** 183–192 (2001)
doi:10.1006/jcis.2001.7827, available online at http://www.idealibrary.com on IDEAL®

Toward the Characterization of Microporosity of Carbonaceous Films

A. P. Terzyk,*,[1] P. A. Gauden,* J. Zawadzki,* G. Rychlicki,* M. Wiśniewski,* and P. Kowalczyk†

*Department of Chemistry, Physicochemistry of Carbon Materials Research Group, N. Copernicus University, Gagarin St. 7, 87-100 Toruń, Poland; and †Department of Respiratory Protection, Military Institute of Chemistry and Radiometry, Gen. Chruściel Avenue 105, 00-910 Warsaw, Poland

Received March 6, 2001; accepted July 11, 2001

Microporous carbon films obtained from cellulose and then chemically modified (oxidation and loading with metal cations, nine samples altogether) are investigated to evaluate their porosity. The materials obtained are microporous; moreover, the majority of micropores possess the same diameter. The results of the calculation of the average pore diameters using different methods based on the analysis of low-temperature nitrogen adsorption data and the measurement of the benzene adsorption isotherm and enthalpy are presented and analyzed. The results obtained with the DFT and HK methods are similar. It is concluded that a good correlation between pore diameters obtained from DFT analysis (for nitrogen adsorption) occurs for those calculated from benzene calorimetry data using the Everett and Powl method and those calculated by applying a recently developed equation.

Key Words: **activated carbon; adsorption; enthalpy; entropy; benzene; carbon films; DA; DFT; HK; microporosity; pore diameter.**

INTRODUCTION

In the application of infrared spectroscopy to surface phenomenon studies, carbon samples prepared from cellulose have considerable utility (1–3). By application of the carbon film technique, the problems of experimental spectroscopic investigations of surface processes on carbon have been solved to a great extent. IR spectroscopic studies of carbonization, oxidation, chemical reactions, adsorption phenomena, and catalytic reactions on carbons prepared from cellulose have been presented elsewhere (4, 5). Carbon films can be used as model substances in investigations of the chemical structures of carbon surfaces and the character of interaction of adsorbed molecules with surfaces (6).

Apart from recording IR spectra, films can be studied using all the other known methods. This paper describes the characterization of the microporosity of carbons, and it will be shown that the carbonization of cellulose, as well as the chemical modification of the carbonization product, leads to the creation of films possessing very interesting features. Moreover, valuable conclusions can be drawn from the comparative analysis of their porosity.

[1] To whom correspondence should be addressed. E-mail: aterzyk@chem.uni.torun.pl.

EXPERIMENTAL

Preparation of Carbon Samples

Carbon samples were prepared from cellulose (1–7). The raw material used for carbonization was cellophane which had previously been purified in 20% HCI and washed repeatedly with distilled water.

The charring experiments were set up as follows: cellulose samples carbonized at 573 K in air for 1 h were evacuated at 873 K for 1 h under dynamic vacuum. The following procedure was used to prepare oxidized carbon samples: The samples outgassed at 873 K (a standard pretreatment) were exposed to 1000 hPa of pure O_2 at 573 K for 1 h and evacuated at 873 K. They were oxidized once more at 573 K and the obtained samples were denoted as C_{ox}. The samples after outgassing at 873 K are denoted as C_{873}.

This film was used as an initial material for achieving metal (Ag, Cu, Ni, Pt)-loaded powdered oxidized carbon samples. They were prepared with an incipient wetness technique using aqueous nitrate solutions as a precursor. The oxidized carbon sample containing Pt was prepared using a 3% solution of H_2PtCl_6. The metal loading level was set at 1%.

All samples were heated in vacuum at 473 K. The obtained samples are denoted as C_{ox}Ag, C_{ox}Cu, C_{ox}Ni, and C_{ox}Pt. Moreover, the sample C_{ox}Cu was desorbed in vacuum at 873 K for 1 h and the obtained sample was denoted as C_{873}Cu. Additionally, a sample with higher Cu content (5%) was obtained, using the procedure described above, and the sample was denoted as C_{ox}Cu5. Finally the effect of grinding the sample C_{ox} was studied and the ground sample was denoted as C_{ox}2.

Measurement of Low-Temperature Nitrogen Adsorption Isotherms

The nitrogen adsorption isotherms were measured at 77.5 K using the ASAP 2010 MicroPore System (Micromeritics, U.S.A.). Before each measurement the carbon samples were desorbed in vacuum at 383 K for 3 h. The molar volume of liquid nitrogen was 34.666 cm^3/mol, and the density was 0.808 g/cm^3 (8).

0021-9797/01 $35.00

Determination of Benzene Adsorption Isotherm and Differential Enthalpy of Adsorption

The benzene adsorption isotherm was measured on carbon C_{ox} at 313.15 K using a volumetric apparatus with Baratron pressure transducers (MKS Instruments, Germany). The desorption of the sample was performed at 383 K until a constant pressure of ca. 10^{-5} Pa was obtained. The measurement of the enthalpy of adsorption, using a Tian–Calvet microcalorimeter, was described in detail previously (9, 10). During the calculation we applied the following benzene constants (8): density = 0.8576 g/cm^3, molar volume of liquid = 91.0798 cm^3/mol, coefficient of thermal expansion of liquid (α) = 0.00116 K^{-1}, and pressure of saturation (p_s) = 242.049 hPa (see the caption for Fig. 7 for some additional data).

RESULTS AND DISCUSSION

Based on the results of low-temperature nitrogen adsorption isotherms (shown on a logarithmic scale in Fig. 1) the structure of the carbons was characterized using the following methods:

- The BET equation (11) (in the range of relative pressure 0.05 up to 0.3) was used to calculate the apparent surface areas S_{BET}.
- The Dubinin–Radushkevich (DR) and/or Dubinin–Astakhov (DA) equations (12) were used to calculate the total micropore volume $W_{0DR/0DA}$. They were applied in the computation of micropore areas (13) $S_{DR/DA}$ ($S_{DR/DA} = 2 \times 10^3 W_{0DR/0DA}/x_{av}$), where x_{av} is the average micropore diameter (calculated in this case by Eq. [6]). DR and DA equations as well as related formulas allow us to calculate the average micropore diameters, and the subsequent equations are presented below (the characteristic energy of adsorption $E_{0DR/0DA}$ and the parameter n of the DA isotherm are used for this purpose).
- The DFT method (14) was used to calculate the total surface area S_{DFT} and pore volume V_{DFT} of investigated samples as well as those parameters for respective types of pores. Thus, for example, the micropore surfaces ($S_{DFT_{micro}}$) and the micropore volumes $V_{DFT_{micro}}$ were calculated for all the pores with diameters smaller and/or equal to 2 nm. Furthermore, the pore size distributions ($J(x)$) were calculated using this method, following the procedure proposed by Olivier and co-workers (15).
- A high-resolution α_s plot (16) was used to calculate the total specific surface area $S_{c,\alpha}$, specific surface area of mesopores $S_{me,\alpha}$, and the volume of micropores $V_{mi,\alpha}$. Graphitized carbon Sterling FT-G (17) was used as a reference system.
- The method of Horvath and Kawazoe (HK) (18) was used to calculate the micropore volumes (V_{HK}) and micropore size distributions ($J(x)$).

The parameters obtained using the above-mentioned methods are shown in Table 1. It can be noticed that the investigated samples possess lower (by about 50%) apparent BET surface areas than typical commercial carbons (19). It can be seen that the total volumes of mesopores, as well as their surface areas,

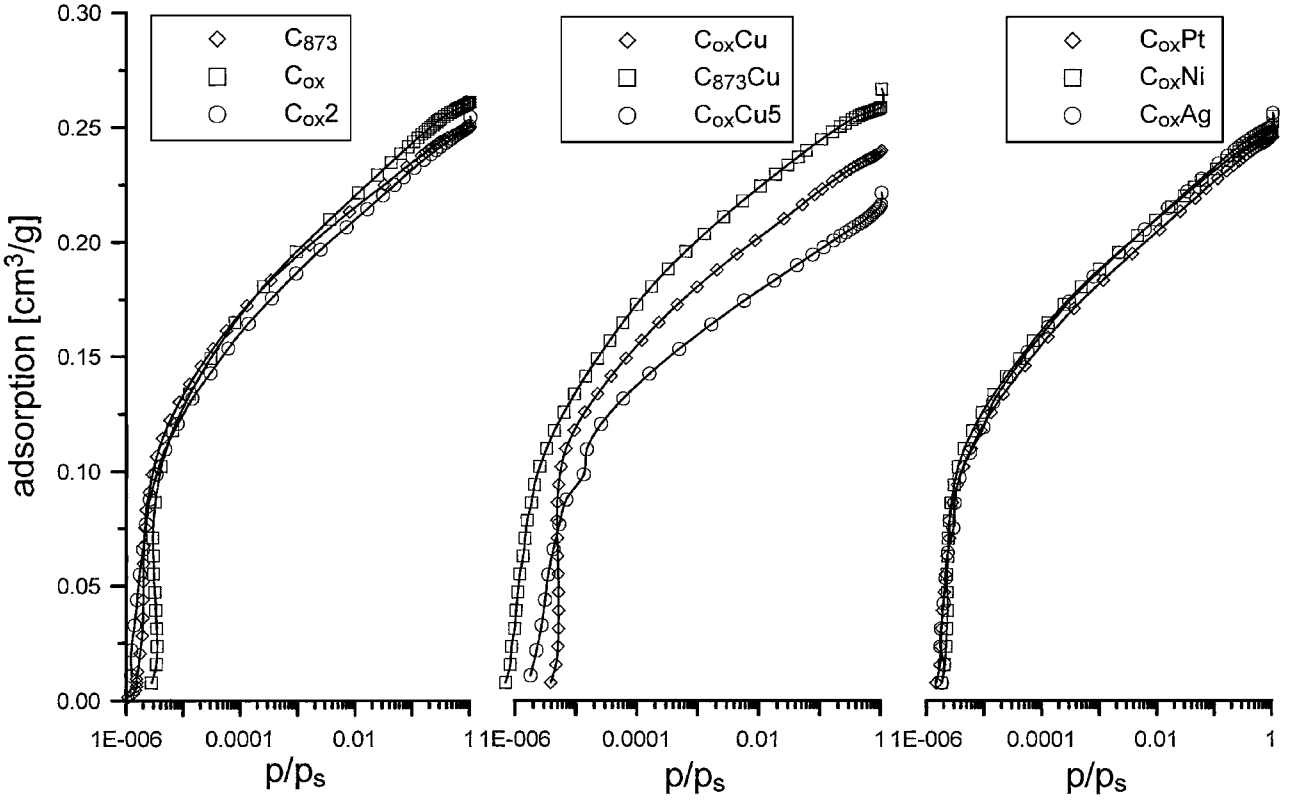

FIG. 1. Nitrogen adsorption isotherms (77.5 K) for the carbonaceous films studied. Note that the logarithmic scale is used for the pressure axis.

TABLE 1
Structural Data

Adsorbent	C_{873}	C_{ox}	$C_{ox}2$	$C_{ox}Cu$	$C_{873}Cu$	$C_{ox}Cu5$	$C_{ox}Pt$	$C_{ox}Ni$	$C_{ox}Ag$
Surfaces areas (m^2/g)									
S_{BET}	478.3	520.1	471.2	449.3	515.2	401.4	461.9	496.8	469.9
S_{DR}	818.9	776.9	761.1	782.1	874.7	877.2	742.5	821.1	765.1
S_{DA}	693.9	671.4	682.8	742.2	797.3	467.7	667.3	767.3	678.6
$S_{DFT_{micro}}$	620.1	941.3	563.9	414.5	675.7	464.8	580.2	647.0	586.9
$S_{DFT_{meso}}$	4.1	8.4	6.0	5.2	2.5	6.5	6.4	4.8	6.0
S_{DFT}	624.2	949.7	569.9	419.7	678.2	471.3	586.6	651.8	592.9
$S_{c,\alpha}$	627.4	661.3	610.1	591.2	646.4	520.3	593.9	610.5	612.6
$S_{me,\alpha}$	2.6	8.2	8.2	7.5	6.8	18.4	9.6	10.5	7.7
Pore volumes (cm^3/g)									
W_{0DR}	0.244	0.251	0.236	0.223	0.247	0.210	0.230	0.232	0.236
W_{0DA}	0.217	0.225	0.220	0.219	0.238	0.177	0.212	0.225	0.220
$V_{DFT,I_{micro}}$	0.178	0.178	0.155	0.135	0.185	0.140	0.162	0.174	0.166
$V_{DFT_{micro}}$	0.192	0.202	0.180	0.165	0.205	0.159	0.185	0.196	0.190
$V_{DFT_{meso}}$	0.005	0.008	0.009	0.010	0.011	0.017	0.010	0.014	0.013
V_{DFT}	0.197	0.210	0.189	0.175	0.216	0.176	0.195	0.210	0.203
V_{HK}	0.239	0.248	0.236	0.241	0.248	0.200	0.231	0.235	0.238
$V_{mi,\alpha}$	0.245	0.247	0.234	0.230	0.251	0.195	0.233	0.234	0.241
Micropore diameters (nm)									
$x_{av,DFT,I}$	0.616	0.536	0.500	0.643	0.536	0.630	0.590	0.537	0.590
$x_{av,DFT,II}$	1.530	1.432	1.345	1.344	1.304	1.427	1.441	1.348	1.384
$x_{av,DFT,tot}$	0.782	0.626	0.598	0.841	0.610	0.677	0.837	0.577	0.738

are very small. Thus, the studied carbons can be regarded as microporous solids.

Generally, the values of surface areas calculated by applying different methods increase after the oxidation of the initial carbon (C_{873}), whereas they decrease for carbons containing metals on the surface, when compared with an oxidized material. Remarkable changes in pore volumes can be observed for carbons containing Cu on the surface. The grinding of C_{ox} leads to a decrease in surface area, while pore volumes, determined by different methods, practically do not change.

The shapes of the high-resolution α_s plots observed for all the studied samples (some arbitrarily chosen samples are shown in Fig. 2) led to the suggestion that the samples are microporous and possess pores where both filling and cooperative swings of nitrogen occur. It can be seen that the linear region is short, indicating the presence of relatively narrow micropores (20). Thus, the FS/CS type of such plots is observed for activated carbons having a bimodal pore size distribution, as was pointed out by Kaneko and co-workers (16). Exactly the same results are obtained on the basis of DFT analysis ($J(x)$); this indicates, for all the studied samples, that the pores are grouped around two main diameters (Figs. 3 and 5, Table 1). The first diameter approaches 0.5–0.6 nm, while the second diameter oscillates in the range of 1.3–1.5 nm. In Table 1 the parameters of the primary and secondary porous structures (determined from DFT) are included. It is shown that the volume of the primary micropores ($V_{DFT,I_{micro}}$) contributes from 82% (carbon $C_{ox}Cu$) up to 93% (carbon C_{873}) of the total volume of micropores (determined from the DFT—cumulative pore size distribution). Thus, the studied films, according to the DFT method, possess an additional interesting and very important feature; i.e., nearly homogeneous microporosity is observed in their structures.

In Figs. 4 and 5 a comparison of the DFT results with those obtained with the HK method is presented. It can be seen that the pore size distribution curves obtained for some cases are very similar, and they cover practically the same ranges of pore diameters; however, they sometimes differ (but the differences are not enormous). Thus, based on strong thermodynamic grounds, the HK method leads, for some studied carbons, to results similar to those obtained using the DFT method. The same conclusions were published by Choma *et al.* (21). They stated that for the series of different activated carbons "two different adsorption methods of the pore-size-distribution determination, mainly DFT and HK, lead to very similar results, and that confirms the validity of the assumptions of HK method as well as its applicability for the determination of microporosity of carbons." One year later Choma *et al.* (22) concluded that "the HK method is not effective for highly microporous carbons and a further improvement of this method is required." The differences between the two methods were also reported by Carrott and co-workers (23), while some similarity was considered by Blacher and coworkers (24). In our opinion, the results presented in this section lead to the statement that for microprous carbons the two methods are similar, and the HK model is, as a matter of fact, the only method of microporosity characterization leading to results similar to those obtained from DFT.

It should be emphasized that there is a problem connected with the comparative analysis of the results of the DFT method

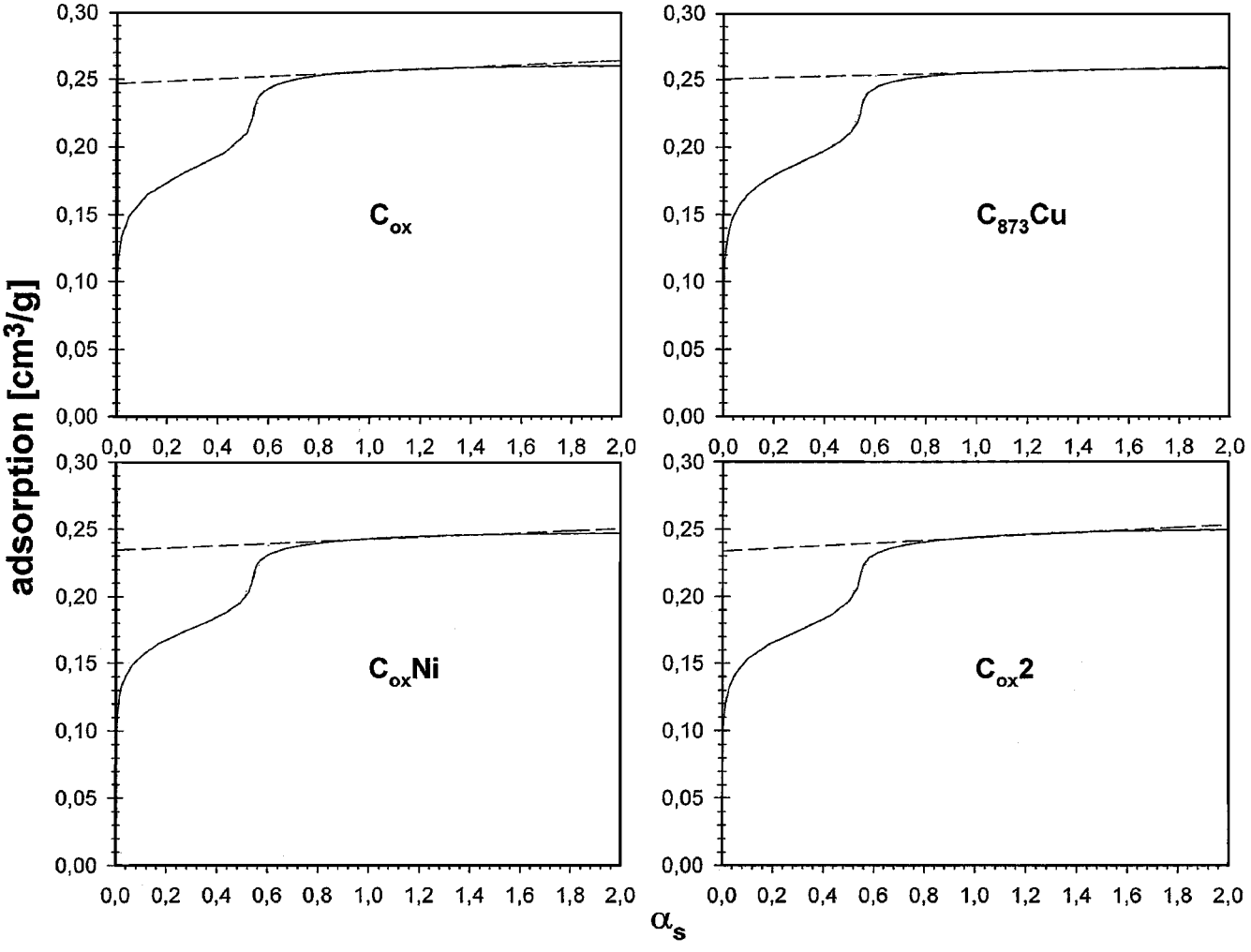

FIG. 2. High-resolution α_s plots obtained using Sterling FT-G graphitized carbon. Only four arbitrarily chosen samples are shown; for all samples the same types of plots, i.e., FS/CS type, are obtained.

and those obtained with the other methods, especially with the methods based on the DR and/or DA equation. The reason is that the empirical equations proposed for the calculation of the average micropore diameters correlate the characteristic energy of adsorption, calculated mainly from the DR equation (see below), with the average width of the slit. The best fit of the DR equation to experimental adsorption data, discussed in the current study, was obtained with the data measured up to a relative pressure of ca. 0.01. Thus, following the mechanism of multistage micropore filling published by Kakei and co-workers (20), only primary micropore filling occurs in this range of the isotherm; which means that the average micropore diameters calculated for this range of adsorption isotherms, obtained using E_0 values, characterize the adsorption process occurring only in the section of the micropores present in the system. Thus, the values of the pore diameters calculated on the basis of this fragment of the isotherm can be compared only with the diameters of the primary micropore structure obtained from DFT analysis, and not with the average pore diameters calculated using this method. That is why the $x_{av,DFT,I}$ and not the average diameters ($x_{av,DFT,tot}$; Table 1) should be taken into account during comparison of the results of microporosity calculation given below. The average micropore diameters were calculated using the results of the most popular equations proposed by

McEnaney and Mays (25, 26),

$$x_{av} = 6.6 - 1.79\ln(E_0) \quad [1]$$

$$x_{av} = 4.691\exp[-0.0666E_0]; \quad [2]$$

Stoeckli *et al.* (27–29),

$$x_{av} = \frac{16.5}{E_0} \quad [3]$$

$$x_{av} = \frac{18}{E_0} \quad [4]$$

$$x_{av} = \frac{10.8}{E_0 - 11.4} \quad [5]$$

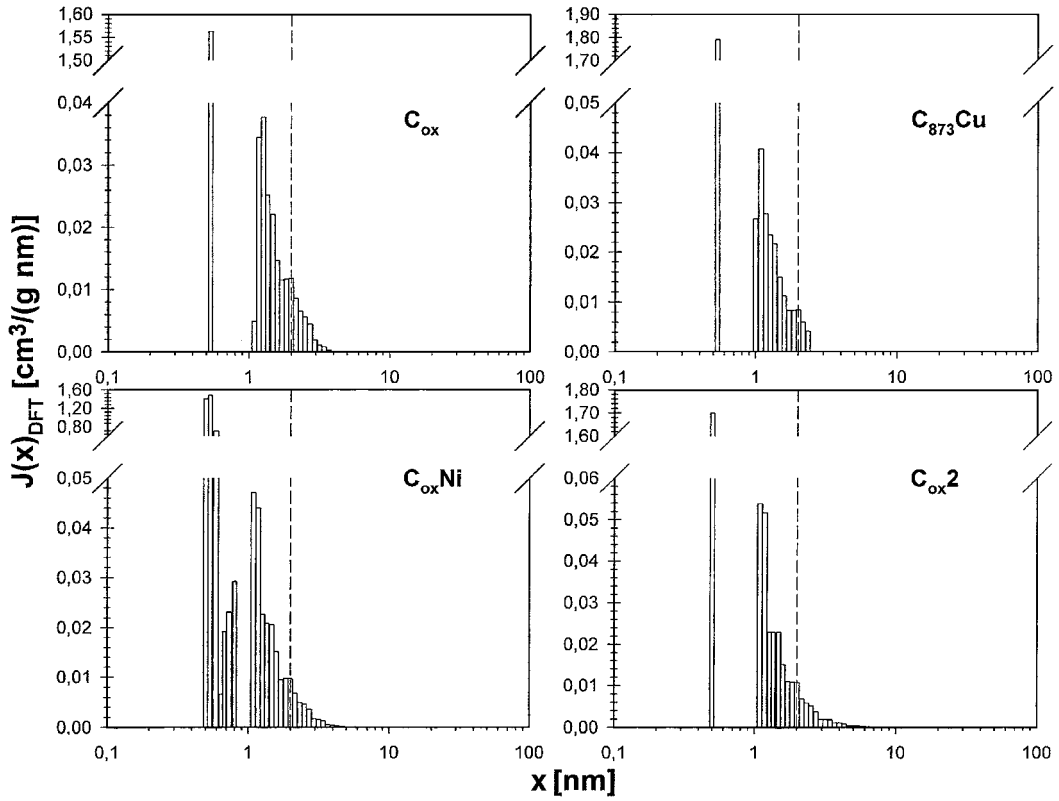

FIG. 3. Differential pore size distributions obtained from the DFT method (only four arbitrarily chosen samples are shown). The vertical dashed line denotes the upper limit of the widths of the micropores.

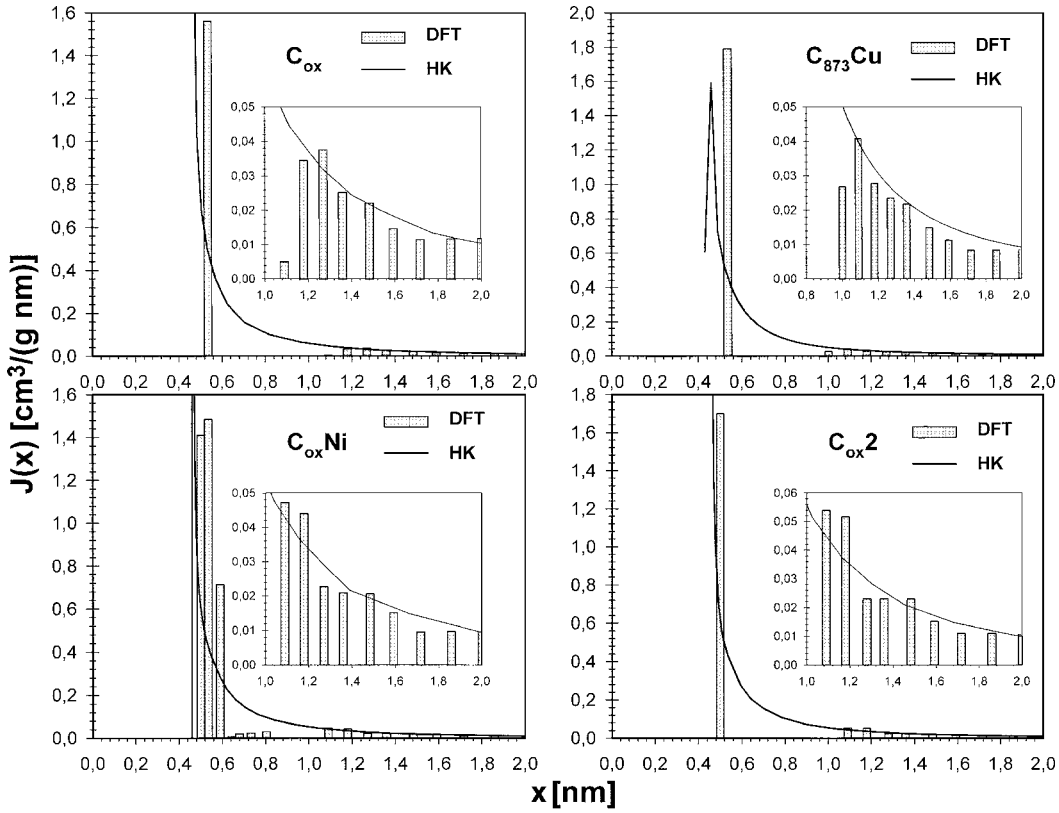

FIG. 4. Comparison of $J(x)$ calculated using the HK and DFT methods. For the samples presented, a relatively good correlation between both methods is observed.

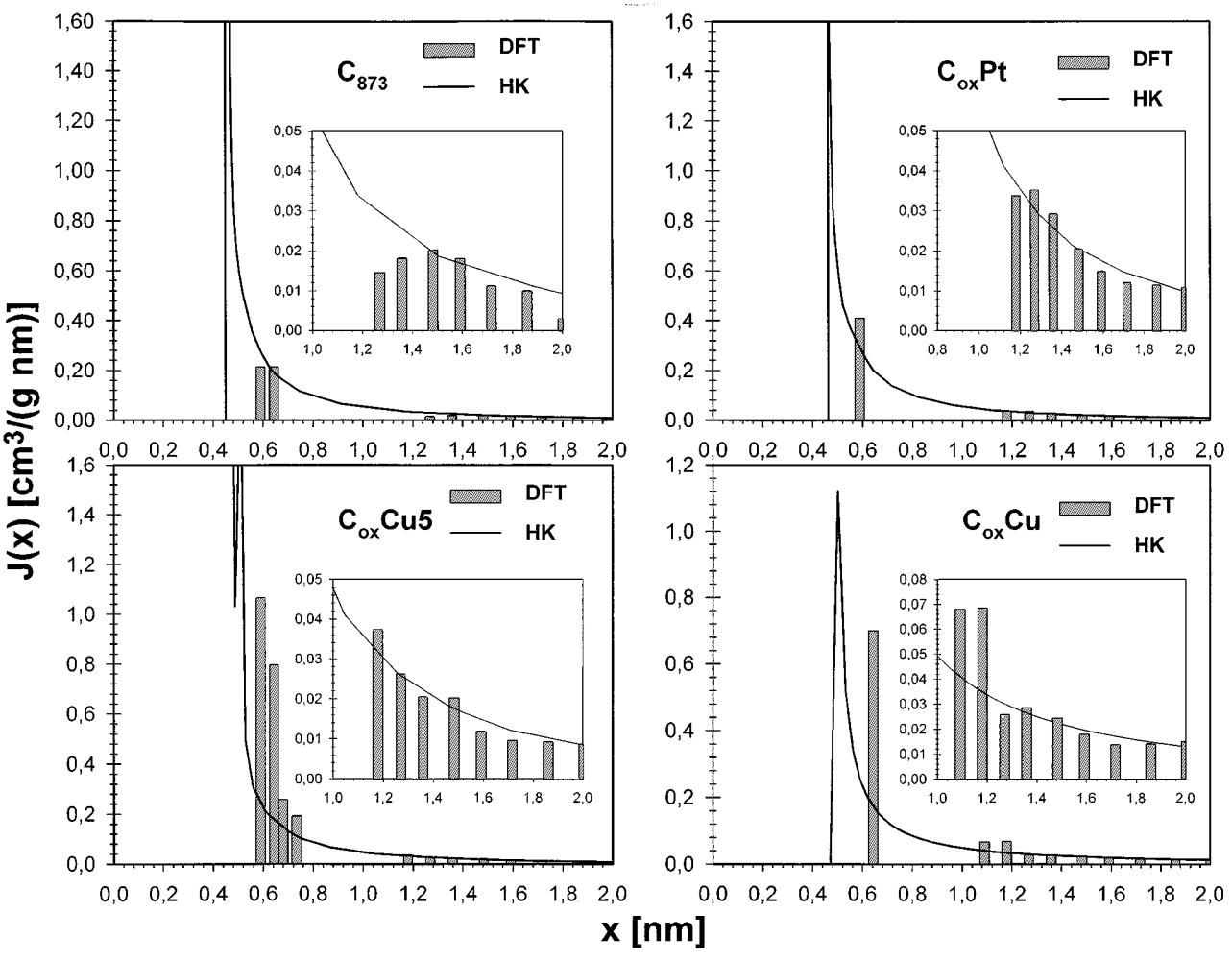

FIG. 5. Comparison of $J(x)$ calculated using HK and DFT methods. For the samples presented, a slightly worse correlation between both methods is observed.

$$x_{av} = \left(\frac{30}{E_0}\right) + \left(\frac{5705}{E_0^3}\right) + 0.028E_0 + 1.49; \quad [6]$$

Choma and Jaroniec (30),

$$x_{av} = \left(\frac{10.416}{E_0}\right) + \left(\frac{13.404}{E_0^3}\right) + 0.008212E_0 + 0.5114; \quad [7]$$

Ohkubo *et al.* (31),

$$x_{av} = \frac{2 \times 10^3 V_{mi,\alpha}}{(S_{c,\alpha} - S_{me,\alpha})}; \quad [8]$$

and more recent authors (32–34),

$$\frac{x_{av}}{d_A} = \frac{a_1}{1 + b_1 \times \exp[-c_1 \times n]} + \frac{a_2 + b_2 \times n + c_2 \times n^2}{E_0}, \quad [9]$$

where d_A is the diameter of an adsorbed molecule (0.3 nm for nitrogen (32–34), 0.459 nm for benzene (35)), $a_1 = 0.7752$, $b_1 = -9.5761$, $c_1 = 2.1227$, $a_2 = 53.7290$, $b_2 = -13.8278$, $c_2 = 1.7692$, and

$$\frac{x_{av(mic)}}{d_A} = \left(\frac{a_{1(mic)} \times n}{b_{1(mic)} + n}\right) \times \left(\frac{a_{2(mic)} \times n}{b_{2(mic)} + n}\right)^{E_0} \times E_0^{\left(\frac{a_{3(mic)} \times n}{b_{3(mic)} + n}\right)}, \quad [10]$$

where $a_{1(mic)} = 24.1672$, $b_{1(mic)} = 2.2709$, $a_{2(mic)} = 0.9960$, $b_{2(mic)} = -1.29 \times 10^{-2}$, $a_{3(mic)} = -0.8586$, $b_{3(mic)} = 1.2266$.

It should be emphasized that Eqs. [1]–[7] were developed on the basis of the correlation of the parameters of Dubinin's isotherm (mainly DR) with different data, obtained usually from independent methods (for example, SAXS), and none of them take into account the parameter n of the DA isotherm. Among the equations presented above, only [9] and [10] take into consideration that n as connected directly to the distribution of the so-called adsorption potential must influence the average diameter of micropores (36–40). Thus, to compare the results of x_{av} calculation the DR equation was fitted to the data of nitrogen

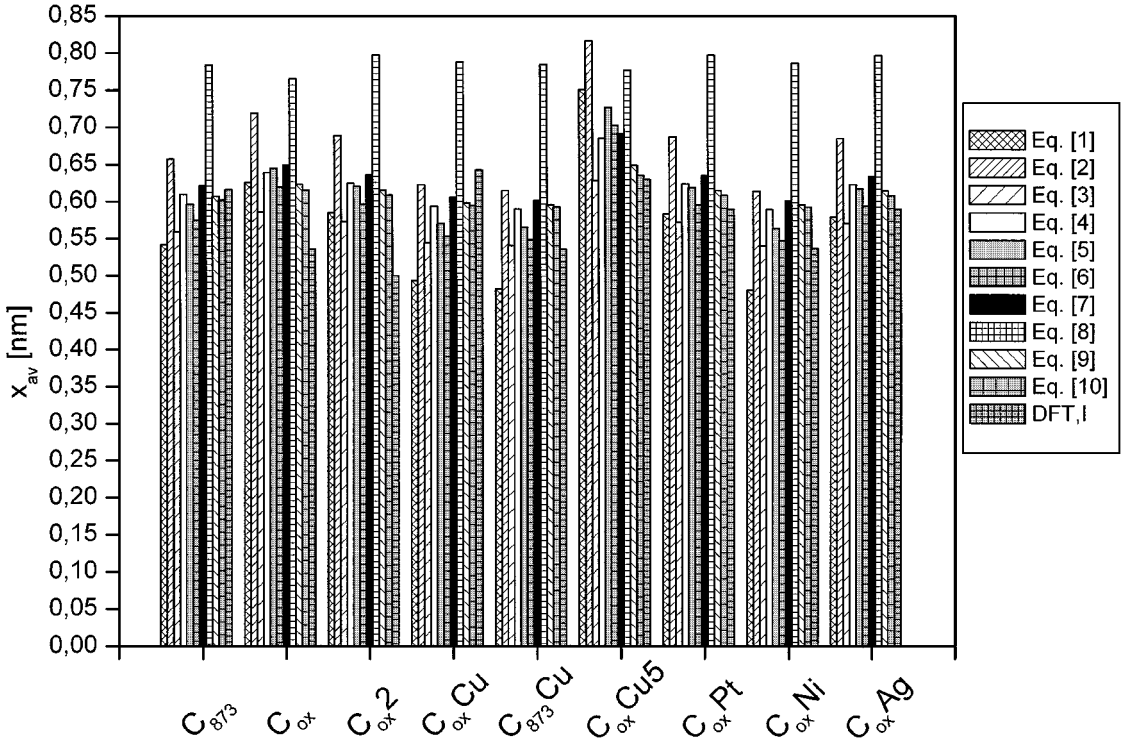

FIG. 6. Comparative plot of average pore diameters obtained from Eqs. [1]–[10] and the DFT method. The primary structure of micropores was considered only because the DR equation was fitted to the range of adsorption which takes place in the pores where micropore filling and no cooperative swings mechanism occur.

adsorption (in Eqs. [9] and [10] $n = 2$ for this case; the fitting using the DA equation leads to almost the same results as those obtained from DR). A comparison of the data obtained is presented in Fig. 6. For all the samples studied, Eq. [8] leads to the highest values of x, while Eq. [1] in most cases leads to the lowest ones. Results similar to DFT are most frequently obtained for Eqs. [3], [10], and [6].

Benzene Adsorption Isotherm and Heat of Adsorption on Carbon C_{ox}

It is well known that the measurement of the enthalpy of adsorption can lead to very interesting information about the mechanism of an adsorption process as well as the energetic and structural heterogeneity of adsorbents (41). We decided to measure, for one of the samples studied, the benzene adsorption isotherm and enthalpy for two reasons: first, to check the thermodynamic validity of the theory of volume filling of micropores, and second, to calculate, using the method published by Everett and Powl (42), the enhancement of potential energy in micropores, in comparison to the energy of adsorption on a "flat" surface. Thus calorimetry can be used as an independent method of indirect determination of the diameter of micropores of a studied carbon. Moreover, benzene was recommended by Dubinin and is widely used as the "standard" adsorbent for the characterization of microporosity. The standard procedure is to measure the benzene adsorption isotherm (usually at around room temperature), to apply the DR and/or DA equation, to determine E_0, and finally to calculate x_{av} using Eqs. [1]–[7].

The data obtained from benzene adsorption as well as the measurements of the heat of adsorption are shown in Fig. 7. In this figure the fitting of the DR and DA isotherm equations to the obtained data is also shown. It can be seen that the DR equation describes the experimental data worse than the DA equation does (the values of the determination coefficients are 0.9149 for DR and 0.9976 for DA, respectively). Using the same procedure as described previously (43), the enthalpy of benzene adsorption was calculated (for the parameters obtained by the fitting of the theoretical adsorption equation to the experimental data) by applying the formalism of the theory of volume filling of micropores (44). However, it should be emphasized that for the carbon sample studied potential theory describes the experimental enthalpy data inadequately; i.e., potential theory equations lead to enthalpy lower than that measured experimentally by about 20 kJ/mol.

Knowing the benzene adsorption isotherm and the differential molar heat of adsorption (q_{diff}), the differential molar entropy of adsorbed molecules (S_{diff}) can be calculated by (10)

$$S_{diff} = S_{\text{g}} - (q_{diff}/T) - R\ln(p/p_0) + R, \qquad [11]$$

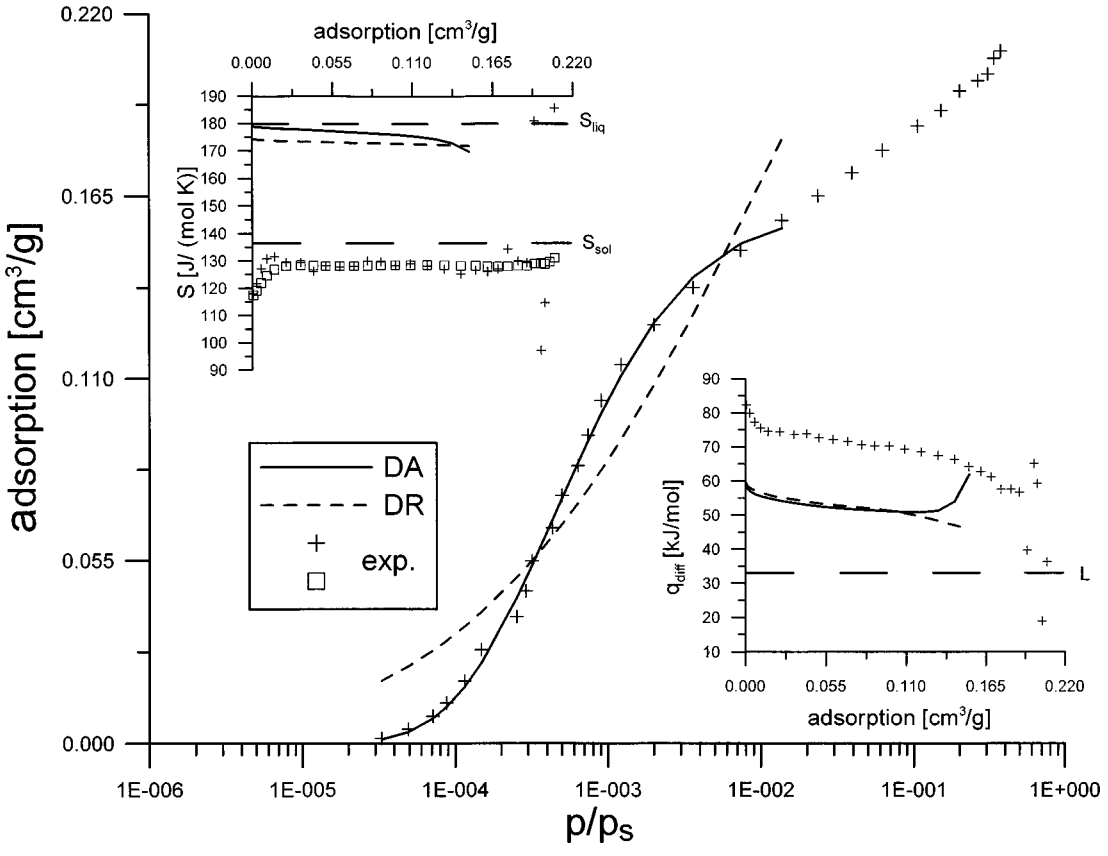

FIG. 7. Experimental data (crosses) measured for benzene and C_{ox} carbon (T = 313.15 K). *Adsorption isotherm*: Line—DA equation (determination coefficient of the fit of adsorption isotherm $DC = 0.9976$, $n = 6.0479$, $E_0 = 20.663$ kJ/mol, $W_0 = 0.159$ cm^3/g). Dashed line—DR equation ($DC = 0.9149$, $n = 2$, $E_0 = 16.215$, $W_0 = 0.292$ cm^3/g). *Entropy*: Line and dashed line as above; crosses—differential molar entropy of adsorbed benzene; squares—integral molar entropy; horizontal dashed lines—the values of the entropy of liquid ($S_{liq} = 179.89$ J/(mol K)) and solid ($S_{sol} = 136.50$ J/(mol K)) benzene. *Enthalpy*: Line and dashed line as above; crosses—differential molar enthalpy measured calorimetrically; horizontal dashed line—the value of the enthalpy of condensation ($L = 33.042$ kJ/mol).

where S_g is the molar entropy of the gas at the temperature T (for benzene at 313.15 K it is equal to 273.08 J/(mol K) (45)), R is the gas constant, and p and p_0 are the equilibrium and the standard state pressure, respectively. It is well known that different standard states can be chosen, and in our case, the gas at the standard pressure of $p_0 = 101{,}325$ Pa was applied. The results are shown in Fig. 7 (it is obvious that a liquid state was taken as a reference during the performance of the calculation following the potential theory). It can be seen that the value of the integral molar entropy of adsorbed benzene falls close to the value characteristic of a solid ($S_{sol} = 136.50$ J/(mol K) (46)). As can be seen from Table 1, 88% of micropores of the studied carbon films possess the same diameter (0.536 nm, and the volume 0.178 cm^3/g—determined from DFT for nitrogen adsorption) and that is why the plot of the integral molar entropy of adsorbed benzene is almost constant (Fig. 7). As can be seen, above adsorption ca. 0.18 cm^3/g an increase in differential entropy occurs, and this is caused by the commencement of adsorption in the secondary structure of pores where differential entropy approaches the value characteristic of a liquid. In this figure the value predicted by potential theory equations is also shown, and as expected this theory leads to too high values of entropy. As shown recently (10, 43) for cases where the adsorbed molecules approach a quasi-solid state, the equations of the potential theory of adsorption do not describe the calorimetric data (usally too low enthalpy values are observed compared to the experimental ones). This leads to the conclusion that the theory of volume filling of micropores needs further development. This problem will be studied in the future.

Knowing that, for a perfect gas and for the standard state of 101,325 Pa, the entropy of benzene is equal to 273.08 J/(mol K) (and the translational entropy contributes 164.10 J/(mol K) to this value), it can be clearly seen that almost all three translational degrees of freedom are lost by adsorbed molecules. Similar effect was observed for adsorption of benzene by a microporous silica (47). We showed recently (10), for the series of adsorbates, that the entropy, as well as the other thermodynamic properties of molecules confined in pores, can approach values characteristic of a quasi-solid. Watanabe and co-workers (48) stated, based on DSC results, that the "liquid" state of benzene confined in micropores should be partially ordered, while the "solid" state should be disordered due to serious geometrical restriction of

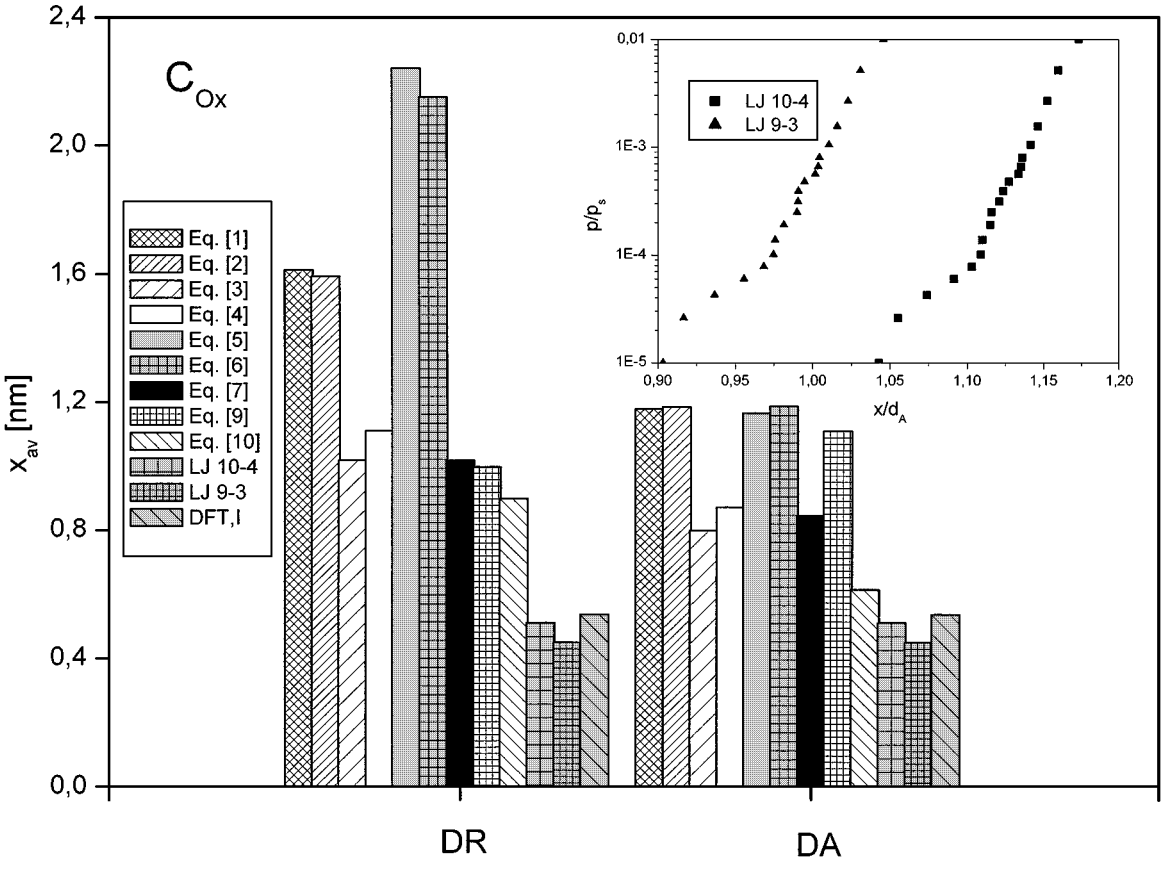

FIG. 8. Comparative analysis of the pore diameters obtained from benzene adsorption and enthalpy data. On the left are the results obtained based on Eqs. [1]–[10] for the DR adsorption equation (in this case $E_{0\mathrm{DR}}$ and $n = 2$ were taken), on the right the results for DA parameters. They are compared with the results calculated using Everett and Powl's method (two potential models were applied) and with those from DFT for nitrogen adsorption ($x_{,\mathrm{DFT,I}}$). The inset presents the results of the calculation using Everett and Powl's method and the enthalpy data measured calorimetrically (Fig. 7).

the formation of a well-crystallized solid structure. Babaev and co-workers (46), who studied the enthalpy of benzene adsorption on an activated carbon AC, reported a similar effect. They noticed a substantial decrease in the entropy of adsorbed benzene from the value characteristic of the enthalpy of a liquid to a value lower than the enthalpy of a solid (the average value of entropy was 155 J/(mol K) and, thus, was located between the value characteristic of a liquid and the entropy of a solid, respectively). In the current study, values of entropy lower than those reported by Babaev and co-workers are observed, and this is caused mainly by the substantial differences in the porosity of the studied samples. The carbon AC studied by those authors possessed mesopores (5% of total volume of pores; their radius calculated on the basis of hysteresis using the Kelvin equation was close to 2 nm); moreover, micropores wider than those of the sample studied in the current paper as, well as a wider dispersion, were observed. Babaev and co-workers (46) noticed that "for the wide distribution of micropores it is impossible to find the fraction of micropores with diameters close to the diameter of benzene molecule, in which adsorbed molecules would lose all the translational and rotational degrees of freedom." The existence of such pores in an investigated sample is confirmed by the analysis of the enhancement of adsorption energy in micropores in comparison with adsorption energy on "flat" surface (graphitized carbon black) calculated from the experimental data of benzene adsorption heat. The enhancement of adsorption energy in micropores (see Fig. 8) was calculated using the value of 43.12 kJ/mol measured by Isirikyan and Kiselev for benzene adsorption on graphitized carbon black MT-1 (49, 50). Thus, following the procedure of Everett and Powl (42), the values of relative pore diameters (x/d_{A}) were calculated for two potential energy models and for the initial range of measured heat assuming, as previously, that the diameter of the benzene molecule (d_{A}) is 0.459 nm (34, 35). Average micropore diameters (average values for the studied relative pressure range was calculated) are shown in Fig. 8, where the comparison with diameters calculated from the parameters of the fit of the DR and DA equations (E_0 and n) with the measured benzene adsorption isotherm is also presented. First, it can be seen that, generally, the diameters obtained from the DR analysis are too high compared with those calculated from enthalpy by the Everett and Powl method. The reason for this could be the poor fitting of the DR equation to

experimental benzene data (this situation does not occur in the case of nitrogen adsorption where both equations lead to similar parameters) (Fig. 7). Therefore, DA parameters are more reliable for this case. Among the relationships studied only Eq. [10] leads to similar average pore diameters, while other relationships lead to a higher values. This is caused mainly by taking into account the value of n in Eq. [10]. The feature of this equation is that x decreases whereas n increases ($n = 6.048$ for this case).

CONCLUSIONS

The method of preparing carbonaceous films presented in this paper leads to the creation of a microporous material with a negligibly small external surface. The FS/CS type of high-resolution α_s plot confirms, as observed in the $J(x)$ curves (in the DFT method), the bimodal structure of micropores.

For these films the pore size distribution curves calculated from the HK method and DFT analysis cover similar (and sometimes exactly the same) ranges of pore diameter. There are no enormous differences between the results of the two methods.

It can be stated that, among the methods of calculating the average micropore diameter studied for nine microporous films, Eqs. [3], [6], and [10] lead to results similar to those obtained from DFT analysis; however, the similarity depends on the type of carbon studied. The applicability of Eq. [10] can be additionally confirmed by examining the results for benzene adsorption obtained with the Everett–Powl method. However, the discrepancy between measured and calculated (using potential theory equations) enthalpy of adsorption (as well as the entropy of adsorbed benzene) describe in this paper leads to the question of how far the values of pore diameters approach the real ones. This question still remains open, especially bearing in mind that the DFT method, which is considered the most sophisticated, has not yet been widely verified thermodynamically for adsorption in microporous systems.

ACKNOWLEDGMENTS

A.P.T. gratefully acknowledges financial support from KBN Grant 3T09A 005 18. P.A.G gratefully acknowledges financial support from KBN Grant 3T09A 150 18.

REFERENCES

1. Zawadzki, J., *Chem. Phys. Carbon* **21,** 147 (1989).
2. Zawadzki, J., Azambre, B., Heintz, O., Krztoń, A., and Weber, J., *Carbon* **38,** 509 (2000).
3. Zawadzki, J., Wiśniewski, M., Weber, J., Heintz, O., and Azambre, B., *Carbon* **39,** 187 (2001).
4. Zawadzki, J., *Carbon* **16,** 491 (1978).
5. Zawadzki, J., *Carbon* **18,** 281 (1980).
6. Zawadzki, J., *Polish J. Chem.* **54,** 979 (1980).
7. Zawadzki, J., *Polish J. Chem.* **52,** 2157 (1978).
8. "Physico-Chemical Handbook." WNT, Warsaw, 1962. [In Polish]
9. Garbacz, J. K., and Rychlicki, G., "Thermodynamics and Calorimetry of an Adsorption Process." UMK, Toruń, 1986. [In Polish]
10. Terzyk, A. P., and Rychlicki, G., *Adsorpt. Sci. Technol.* **17,** 323 (1999).
11. Brunauer, S., Emmett, P. H., and Teller, E., *J. Am. Chem. Soc.* **60,** 309 (1938).
12. Dubinin, M. M., and Astahov, V. A., *Izv. Akad. Nauk. SSSR* **1,** 5 (1971).
13. Stoeckil, F., Huguenin, D., and Laederach, A., *Carbon* **32,** 1359 (1994).
14. Seaton, N. A., Walton, J. P. R. B., and Quirke, N. A., *Carbon* **27,** 853 (1989).
15. Olivier, J. P., Conklin, W. B., and Von Szombathley, M., *Stud. Surf. Sci. Catal.* **87,** 81 (1994).
16. Kaneko, K., Ishii, C., Kanoh, H., Hanzawa, Y., Setoyama, N., and Suzuki, T., *Adv. Colloid Interface Sci.* **76–77,** 295 (1998).
17. Choma, J., and Jaroniec, M., *Polish J. Chem.* **71,** 380 (1997).
18. Horvath, G., and Kawazoe, K., *J. Chem. Eng. Jpn.* **16,** 6 (1983).
19. Rychlicki, G., Terzyk, A. P., and Majchrzycki, W., *J. Chem. Technol. Biotechnol.* **74,** 329 (1999).
20. Kakei, K., Ozeki, S., Suzuki, T., and Kaneko, K., *J. Chem. Soc., Faraday Trans.* **86,** 371 (1990).
21. Choma, J., Jaroniec, M., and Olivier, J. P., *Przem. Chem.* **76,** 101 (1997).
22. Choma, J., and Jaroniec, M., *Polish J. Appl. Chem.* **XL,** 363 (1996).
23. Carrott, P. J. M., Ribeiro Carrott, M. M. L., and Mays, T. J., *in* " Proc. 7th Int. Conf. Fundam. Adsorpt," p. 677. Elsevier, Paris, 1988.
24. Blacher, S., Sahouli, B., Heinrichs, B., Lodewyckx, P., Pirard, R., and Pirard, J. P., *Langmuir* **16,** 6754 (2000).
25. McEnaney, B., *Carbon* **25,** 69 (1987).
26. McEnaney, B., and Mays, T. J., *in* "COPS II Conference." Alicante, 1990.
27. Stoeckli, H. F., *Carbon* **28,** 1 (1990).
28. Stoeckli, H. F., Huguenin, D., and Laederach, A., *Carbon* **32,** 1359 (1994).
29. Stoeckli, H. F., Ballerini, L., and De Bernardi, A., *Carbon* **27,** 501 (1989).
30. Choma, J., and Jaroniec, M., *Karbo-Energochem.-Ekol.* **11,** 368 (1997). [In Polish]
31. Ohkubo, T., Iiyama, T., Nishikawa, K., Suzuki, T., and Kaneko, K., *J. Phys. Chem.* **103,** 1859 (1999).
32. Terzyk, A. P., Gauden, P. A., Rychlicki, G., and Wojsz, R., *Carbon* **36,** 1703 (1998).
33. Terzyk, A. P., Gauden, P. A., Rychlicki, G., and Wojsz, R., *Carbon* **37,** 539 (1999).
34. Terzyk, A. P., and Gauden, P. A., *Colloids. Surf. A.* **57,** 177 (2001).
35. Clifton, B., and Cosgrove, T., *Mol. Phys.* **93,** 767 (1998).
36. Ozawa, A., Kusumi, S., and Ogino, Y., *J. Colloid Interface Sci.* **56,** 83 (1976).
37. Rand, B., *J. Colloid Interface Sci.* **56,** 337 (1976).
38. Bansal, R. C., Donnet, J. B., and Stoeckli, H. F., "Active Carbon." Dekker, New York/Basel, 1988.
39. Rudziński, W., and Everett, D. H., "Adsorption of Gases on Heterogeneous Surfaces." Academic Press, London, 1992.
40. Błażewicz, S., Świątkowski, A., and Trznadel, B. J., *Carbon* **37,** 693 (1999).
41. Rychlicki, G., and Terzyk, A. P., *J. Therm. Anal.* **45,** 961 (1995).
42. Everett, D. H., and Powl, J. C., *J. Chem. Soc., Faraday Trans.* **72,** 619 (1976).
43. Rychlicki, G., and Terzyk, A. P. *Adsorption Sci. Technol.* **16,** 8 (1988).
44. Dubinin, M. M., "Adsorption and Porosity." WAT, Warsaw, 1975. [In Polish]
45. Landolt–Bornstein, "Zahlenwerte und Funktionen." Springer-Verlag, Berlin, 1961.
46. Babaev, P. I., Dubinin, M. M., and Isirikyan, A. A., *Izv. Akad. Nauk. SSSR* **9,** 1929 (1976).
47. Pendleton, P., *J. Colloid Interface Sci.* **227,** 227 (2000).
48. Watanabe, A., Iiyama, T., and Kaneko, K., *Chem. Phys. Lett.* **305,** 71 (1999).
49. Isirikyan, A. A., and Kiselev, A. V., *J. Chem. Phys.* **65,** 601 (1961).
50. Isirikyan, A. A., and Kiselev, A. V., *J. Chem. Phys.* **66,** 210 (1962).